Journal of Vacuum Science and Technology A

RESEARCH ARTICLE | FEBRUARY 14 2024

Selective and nonselective plasma etching of $(Al_{0.18}Ga_{0.82})_2O_3$/$Ga_2O_3$ heterostructures

Special Collection: Gallium Oxide Materials and Devices

Hsiao-Hsuan Wan ; Chao-Ching Chiang ; Jian-Sian Li ; Fan Ren ; Fikadu Alema ; Andrei Osinsky ; Stephen J. Pearton

J. Vac. Sci. Technol. A 42, 022603 (2024)
https://doi.org/10.1116/6.0003400

JVST A
Journal of Vacuum Science & Technology A

ARTICLE

pubs.aip.org/avs/jva

Selective and nonselective plasma etching of $(Al_{0.18}Ga_{0.82})_2O_3$/ Ga_2O_3 heterostructures

Cite as: J. Vac. Sci. Technol. A **42**, 022603 (2024); doi: 10.1116/6.0003400
Submitted: 17 December 2023 · Accepted: 22 January 2024 ·
Published Online: 14 February 2024

Hsiao-Hsuan Wan,[1,a)] Chao-Ching Chiang,[1] Jian-Sian Li,[1] Fan Ren,[1] Fikadu Alema,[2] Andrei Osinsky,[2] and Stephen J. Pearton[3]

AFFILIATIONS

[1]Department of Chemical Engineering, University of Florida, Gainesville, Florida 32611
[2]Agnitron Technology Inc., Chanhassen, Minnesota 55317
[3]Department of Material Science and Engineering, University of Florida, Gainesville, Florida 32611

Note: This paper is part of the Special Topic Collection on Gallium Oxide Materials and Devices.
[a)]**Electronic mail:** hwan@ufl.edu

ABSTRACT

The addition of CHF_3 to Cl_2/Ar inductively coupled plasmas operating at low dc self-biases (<100 V, corresponding to incident ion energies <125 eV) leads to etch selectivity for Ga_2O_3 over $(Al_{0.18}Ga_{0.82})_2O_3$ of >30, with a maximum value of 55. By sharp contrast, without CHF_3, the etching is nonselective over a large range of source and rf chuck powers. We focused on low ion energy conditions that would be required for device fabrication. This result has a direct application to selective removal of Ga_2O_3 contact layers to expose underlying $(Al_{0.18}Ga_{0.82})_2O_3$ donor layers in high-electron-mobility transistor structures. It is expected that formation of nonvolatile AlF_3 species helps produce this selectivity. X-ray photoelectron spectroscopy does detect F residues on the etched surface for the Cl_2/Ar/ CHF_3 plasma chemistry.

I. INTRODUCTION

The ternary alloy $(Al_xGa_{1-x})_2O_3$ demonstrates utility in modulation-doped transistors featuring high-electron-density channels formed at the interface with Ga_2O_3.[1–12] Additionally, in its polycrystalline form, it serves as a transparent conducting oxide.[13,14] The alloy has also gained considerable prominence in the domains of optoelectronics and transparent electronics owing to its noteworthy electrical conductivity and optical transparency. Its potential application extends to serving as a deep ultraviolet (UV) transparent film for optoelectronic devices.

In terms of fabricating High-Electron-Mobility Transistors (HEMTs) based on the $(Al_xGa_{1-x})_2O_3$/ Ga_2O_3 heterostructure, one of the key steps is selective removal of a Ga_2O_3-doped contact layer from the underlying $(Al_{0.18}Ga_{0.82})_2O_3$ donor layer, allowing deposition of rectifying contact.[9] This step needs high selectivity removal of Ga_2O_3 and low damage to the $(Al_xGa_{1-x})_2O_3$ layer. Complicating this is the fact that the Al composition in the ternary layer is generally relatively low, in the range of 0.17–0.22.[1,3,5–7,12] For manufacturing purposes, a minimum selectivity of at least 10 is desirable.[9] The predominant methodology for the $(Al_xGa_{1-x})_2O_3$ /Ga_2O_3 patterning involves dry etching due to the inherent absence of wet etching capabilities at room temperature, as documented in various studies.[15–24] The extent of ion-induced damage under practical etching conditions has been reported previously, with alterations in the electrical properties of the etched surface observed to extend beyond the spatial range of incident ions.[25–27] This phenomenon is commonly attributed to the rapid diffusion of primary defects, such as vacancies or interstitials.[25–28]

Differential etching rates or selectivity between two distinct layers arise from variations in the volatility of their respective etch byproducts or the development of an etch-stop material on the surface.[26] A representative instance is the utilization of Cl_2/SF_6 for the selective etching of GaAs in preference to AlGaAs[26,29,30] and also GaN over AlGaN.[31] In this scenario, selectivity is established through the generation of nonvolatile AlF_3 on the AlGaAs or AlGaN surfaces subsequent to the etching of GaAs or GaN, respectively. Analogously, a comparable outcome can be achieved by introducing oxygen into a chlorine plasma to generate AlOx species on the AlGaAs or AlGaN surfaces.[26,30,31] The selectivity

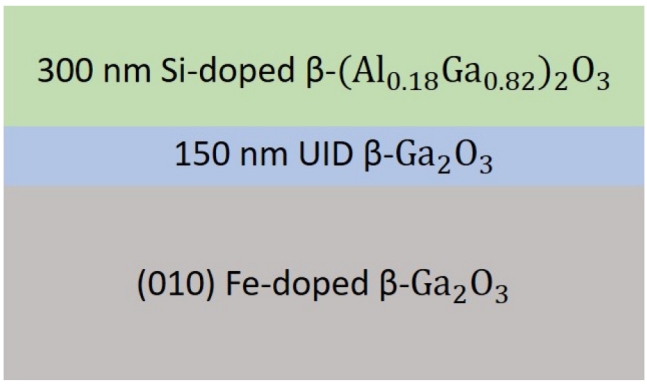

FIG. 1. Schematic of the structure of $(Al_{0.18}Ga_{0.82})_2O_3$ in this study.

mechanism is predominantly governed by chemical processes, demonstrating a pronounced sensitivity to incident ion energy and flux. High-density plasmas typically exhibit lower selectivities than their reactive ion etching (RIE) counterparts.[26] Conventional etch-stop reactions, such as the formation of AlF_3, may be less effective, potentially resulting in premature passivation. In the case of achieving selective etching of Ga_2O_3 over $(Al_xGa_{1-x})_2O_3$ at low Al contents, the strategy is to add F_2 or O_2 to the plasma chemistry to form nonvolatile etch products. In this work, we have chosen a source of F to avoid deleterious oxidation effects on the $(Al_xGa_{1-x})_2O_3$ donor layer. Fluorine incorporation into Si-doped Al-containing semiconductors causes reduction in carrier density, and this effect has been used to control the threshold voltage in transistors through compensating Si donors with the negatively charged F ions.[32–36] The fluorine can be incorporated during exposure to wet chemical solutions such as HF, by direct implantation of low-energy fluorine ions or by immersion in a fluorine-containing plasma, including in Ga_2O_3.[35] Avoiding this F-induced donor compensation is important for maintaining the electrical characteristics of Ga_2O_3.

II. EXPERIMENTAL

0.3 μm thick, silicon-doped, n-type (4.1×10^{19} cm^{-3}) $(Al_{0.18}Ga_{0.82})_2O_3$ layers were employed in the conducted experiments. These specimens were grown via Metal Organic Vapor Phase Epitaxy within an Agnitron Technology Agilis 100 MOVPE reactor, utilizing insulating (010) β-Ga_2O_3: Fe substrates. The layers were synthesized at approximately 600 °C on an unintentionally doped Ga_2O_3 buffer layer with a thickness of approximately 150 nm. The precursors employed in the process included triethylgallium, trimethylaluminum, O_2, with SiH_4 serving as the dopant gas and Ar as the carrier gas. A detailed description of the growth methodology has been provided previously.[2,37] The epitaxial structure is depicted in the schematic representation of Fig. 1. The β-Ga_2O_3 samples for etch rate measurements were (100) bulk, Sn-doped substrates, grown by the Edge-Fed Defined Growth method and purchased from Novel Crystal Technology (Saitama, Japan).

The etching was conducted using a PlasmaTherm 790 Inductively Coupled Plasma reactor. Etching was performed under the following conditions: discharges of 15 SCCM of Cl_2 and 5 SCCM of Ar, sometimes with the addition of 5 SCCM CHF_3 at a fixed pressure of 5 mTorr. The ICP source power and rf chuck power were systematically varied to manipulate plasma density and ion energy, respectively, thereby influencing the etch rates. The etching was nominally performed at room temperature with the samples connected to the water-cooled platen with thermal grease. Given the short etch times, we do not expect a significant temperature rise and there was no evidence of thermal degradation of the resist masks. Etch rates were determined by assessing the etch depth using a Tencor profilometer after the removal of the photoresist. Notably, brief plasma exposures lasting approximately 1–2 min did not result in significant surface roughening. The samples were lithographically pattered using AZ 4620 photoresist with a thickness of ~1 μm. All of the etch processes were done at room temperature. Etch time was 2 min. Etch depth and surface root mean square (RMS) roughness of the processed samples were measured with a surface profilometer (Tencor alpha-step IQ).

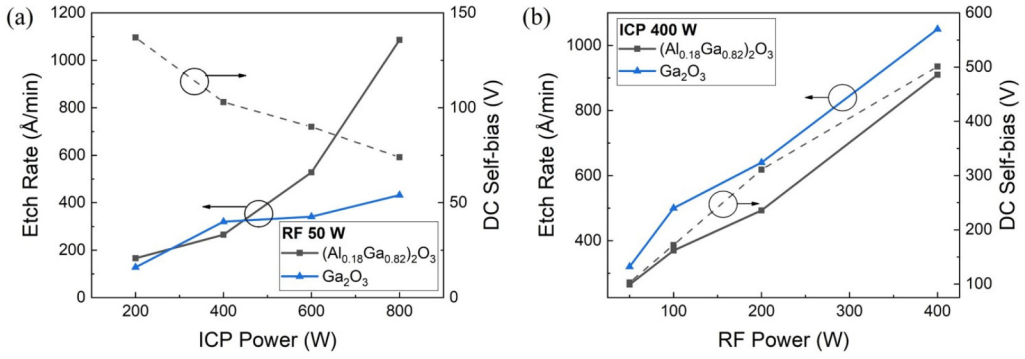

FIG. 2. ICP dry etch rates of $(Al_{0.18}Ga_{0.82})_2O_3$ and Ga_2O_3 in 15 SCCM Cl_2/5 SCCM Ar discharges as a function of (a) ICP power at a fixed RF source power of 50 W. (b) RF source power at a fixed ICP power of 400 W. The DC self-bias is indicated in both cases.

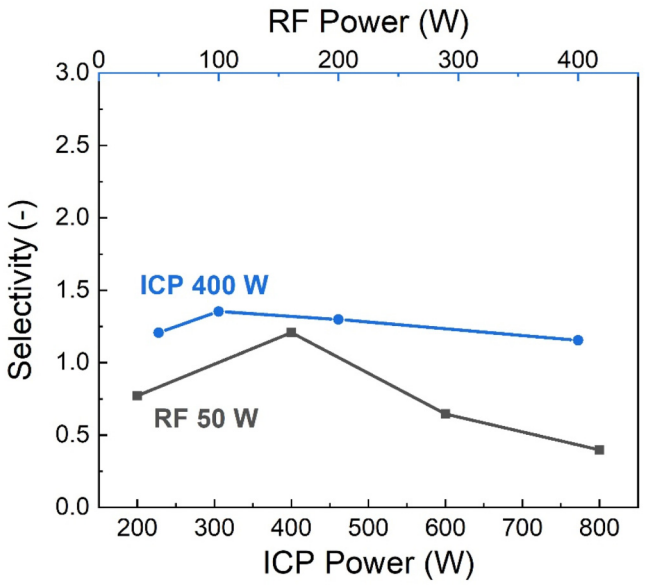

FIG. 3. Selectivity for dry etching of Ga_2O_3 over $(Al_{0.18}Ga_{0.82})_2O_3$ in 15 SCCM Cl_2/5 SCCM Ar discharges as a function of either RF power or ICP source power.

The x-ray photoelectron spectroscopy (XPS) system utilized in this study was a Physical Instruments ULVAC PHI instrument, equipped with an aluminum (Al) x-ray source characterized by an energy of 1486.6 electron volts (eV) and a source power of 300 W. The analysis parameters included a spot size of 100 μm in diameter, a take-off angle of 50°, and an acceptance angle of ±7°. For high-resolution scans, the electron pass energy was set at 23.5 eV, while for survey scans, it was set at 93.5 eV. The overall energy resolution of the XPS system was approximately 0.5 eV, and the observed binding energy exhibited an accuracy within 0.03 Ev.

III. RESULTS AND DISCUSSION

Figure 2(a) shows the etch rates of $(Al_{0.18}Ga_{0.82})_2O_3$ and Ga_2O_3 in 15 SCCM Cl_2/5 SCCM Ar discharges as a function of ICP power at a fixed RF source power of 50 W. Figure 2(b) shows the etch rates as a function of RF source power at a fixed ICP power of 400 W. The DC self-bias is indicated in both cases. This parameter increases with rf power due to increased ionization of the gas in the plasma, leading to a higher density of charged particles.[26] This increased charge density can contribute to a higher self-bias voltage. By contrast, increasing ICP source power typically leads to a higher electron density in the plasma. Higher electron density means more efficient ionization of the gas in the plasma. Increased ionization can result in a higher density of positive ions in the plasma, which can reduce the sheath potential and, consequently, the DC self-bias voltage.[26] The self-bias voltage refers to the DC voltage that develops across the sheath of a plasma discharge. The sheath is a thin layer of plasma near the electrode where the electric field is concentrated. The resultant average ion energy is the sum of the dc self-bias and the plasma sheath potential.[25] The latter is ~23 V under the conditions used in the experiments.[25] Therefore, the ion energies range from ~73 to 523 eV over the range of conditions we examined. There is little selectivity between the etch rates of Ga_2O_3 and $(Al_{0.18}Ga_{0.82})_2O_3$ under any conditions in the Cl_2/Ar discharges.

Figure 3 shows the resultant selectivities for dry etching of Ga_2O_3 over $(Al_{0.18}Ga_{0.82})_2O_3$ in Cl_2/ Ar discharges as a function of either RF power or ICP source power. These are in the range 0.5–1.3 and are well short of practical values.

The effect of addition of CHF_3 to promote an etch stop reaction is shown in Fig. 4, where the etch rates are given of (a) $(Al_{0.18}Ga_{0.82})_2O_3$ and (b) Ga_2O_3 in 15 SCCM Cl_2/ 5 SCCM Ar/ 5 SCCM CHF_3 discharges as a function of ICP power at a fixed RF source power of 50 W. The rates of the alloy decrease significantly with the addition of trifluoromethane for this low rf power condition. By contrast, the etch rate of the Ga_2O_3 increases with this addition, possibly because methyl-based products are formed that add to the removal rate of $GaCl_x$ products, particularly at high ICP source powers.

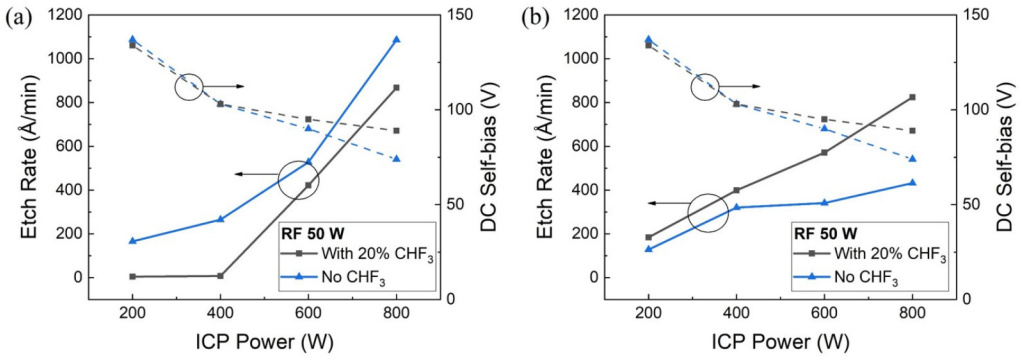

FIG. 4. ICP dry etch rates of (a) $(Al_{0.18}Ga_{0.82})_2O_3$ and (b) Ga_2O_3 in 15 SCCM Cl_2/5 SCCM Ar/CHF_3 5 SCCM discharges as a function of ICP power at a fixed RF source power of 50 W. The DC self-bias is indicated in both cases.

The resultant etch selectivities for dry etching of Ga_2O_3 over $(Al_{0.18}Ga_{0.82})_2O_3$ in $Cl_2/Ar/CHF_3$ discharges are shown in Fig. 5 as a function of ICP power at a fixed rf power of 50W. Very high selectivities >30 are obtained at moderate ICP source powers, with a maximum value of 55. The incident ion energies are ~100 eV under these conditions, making them ideal for low damage removal of a Ga_2O_3 contact layer to expose the underlying ternary for deposition of the gate contact. We only did limited experiments with varying the CHF_3 ratio at a fixed rf or ICP power, but the selectivity was already increased to values >30 even at low CHF_3 additions. This is not surprising given the low total flow rate of all the gases. We did not increase the CHF_3 flow rate above 5 SCCM to avoid excessive polymerization within the chamber.

It is also worth noting that additional OES data to understand the chemistry of the plasma would be useful, although these chemistries are common in selective dielectric etching in semiconductor technology, and balancing the etch and deposition is crucial.

Figure 6 shows XPS data from the ternary alloy before and after exposure to either Cl_2/Ar or $Cl_2/5$ Ar/CHF_3 discharges. There are clearly F residues remaining on the etched surface in the latter case, which promotes the etch stop reaction. The formation of AlF_3 is always the dominant factor in obtaining selective etching of the Ga-dominant alloy relative to the Al-containing alloy.[26,29–31] F can be removed by standard RCA-type wet cleaning. There is no residual polymer on the surface from the XPS data, with the carbon bonded to itself or oxygen. In addition, the formation of GaF_3 would retard the etch rate of Ga_2O_3 by essentially the same amount as for the AGO. Our experience with producing selective etching in the GaAs/AlGaAs and GaN/AlGaN systems by addition of F-containing gases (usually SF_6) suggests that it is reasonable to infer the same mechanism as proven in those systems.[29–31] Note also that under these plasma conditions, there is significant dissociation of atomic fluorine from CHF_3.[38] This tool shows the usual series of F atomic lines from 623.9 to 775.4 nm, far more prominent than the CF_X lines in the 203–388.3 range. The XPS is not consistent with polymer deposition. C is only bonded to itself and oxygen.

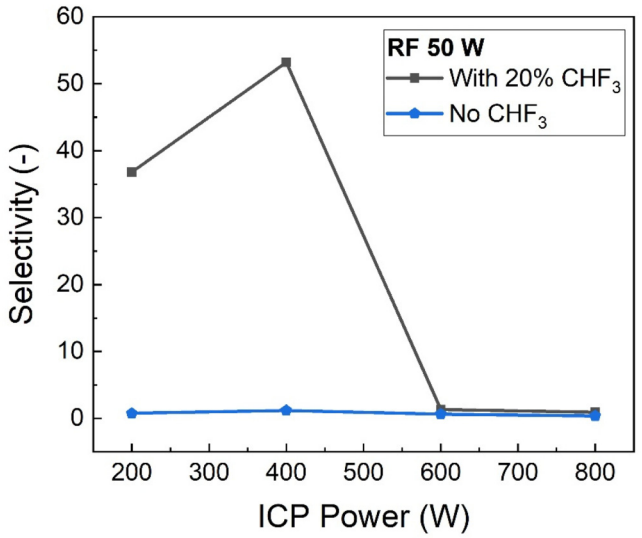

FIG. 5. Selectivity for dry etching of Ga_2O_3 over $(Al_{0.18}Ga_{0.82})_2O_3$ in 15 SCCM Cl_2/5 SCCM Ar/5 SCCM CHF_3 discharges as a function of ICP source power at a fixed RF source power of 50 W.

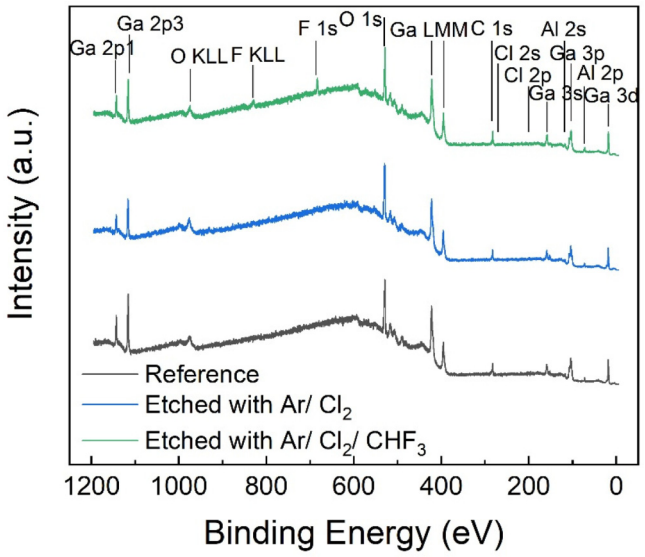

FIG. 6. Survey XPS spectra from $(Al_{0.18}Ga_{0.82})_2O_3$ before and after exposure to the Ar/ Cl_2/ CHF_3 discharge.

Finally, we note there was no change in the sheet carrier density of the films after the selective dry etch process, indicating no significant incorporation of F ions into the material.

IV. SUMMARY AND CONCLUSIONS

High dry etch selectivities are achieved for Ga_2O_3 over $(Al_{0.18}Ga_{0.82})_2O_3$ in $Cl_2/Ar/CHF_3$ discharges at low rf electrode powers and moderate ICP source powers. The CHF_3 addition is the key to enhancing the selectivity. Under most conditions with Cl_2/Ar plasma chemistries, the etching is nonselective. These results provide a simple ICP chemistry for selective and nonselective patterning of $Ga_2O_3/(Al_{0.18}Ga_{0.82})_2O_3$ heterostructures. Achieving high selectivity would become easier at higher Al contents. In addition, another route that could be explored is the use of other C-free, fluorine sources such as SF_6, NF_3, or other gases. These provide F concentrations without the addition of carbon. There was no additional roughening of the surface for the selective etch condition. Similarly, under our pressure and gas flow rate conditions, polymer deposition within the chamber was negligible for the duration of the experiments.

ACKNOWLEDGMENTS

This research was performed as part of the Interaction of Ionizing Radiation with Matter University Research Alliance

(IIRM-URA), sponsored by the Department of the Defense, Defense Threat Reduction Agency under Award No. HDTRA1-20-2-0002. The content of the information does not necessarily reflect the position or the policy of the federal government, and no official endorsement should be inferred. This work at UF was also supported by NSF DMR No. 1856662.

AUTHOR DECLARATIONS

Conflict of interest

The authors have no conflicts to disclose.

Author Contributions

Hsiao-Hsuan Wan: Conceptualization (equal); Data curation (equal); Formal analysis (equal); Investigation (equal); Methodology (equal); Validation (equal); Visualization (equal); Writing – original draft (equal). **Chao-Ching Chiang:** Data curation (equal); Investigation (equal); Methodology (equal); Validation (equal). **Jian-Sian Li:** Conceptualization (equal); Data curation (equal). **Fan Ren:** Conceptualization (equal); Funding acquisition (equal); Project administration (equal); Resources (equal); Supervision (equal); Writing – review & editing (equal). **Fikadu Alema:** Conceptualization (equal); Formal analysis (equal); Funding acquisition (equal); Resources (equal); Writing – review & editing (equal). **Andrei Osinsky:** Conceptualization (equal); Formal analysis (equal); Funding acquisition (equal); Resources (equal); Writing – review & editing (equal). **Stephen J. Pearton:** Conceptualization (equal); Funding acquisition (equal); Methodology (equal); Project administration (equal); Supervision (equal); Writing – review & editing (equal).

DATA AVAILABILITY

The data that support the findings of this study are available within the article.

REFERENCES

[1]E. Ahmadi, O. S. Koksaldi, X. Zheng, T. Mates, Y. Oshima, U. K. Mishra, and J. S. Speck, Appl. Phys. Express **10**, 071101 (2017).
[2]F. Alema, C. Peterson, A. Bhattacharyya, S. Roy, S. Krishnamoorthy, and A. Osinsky, IEEE Electr. Device L. **43**, 1649 (2022).
[3]C. Joishi, Y. Zhang, Z. Xia, W. Sun, A. R. Arehart, S. Ringel, S. Lodha, and S. Rajan, IEEE Electr. Device L. **40**, 1241 (2019).
[4]N. K. Kalarickal, Z. Xia, H.-L. Huang, W. Moore, Y. Liu, M. Brenner, J. Hwang, and S. Rajan, IEEE Electr. Device Lett. **42**, 899 (2021).
[5]N. K. Kalarickal, Z. Xia, J. F. McGlone, Y. Liu, W. Moore, A. R. Arehart, S. A. Ringel, and S. Rajan, J. Appl. Phys. **127**, 215706 (2020).
[6]S. Krishnamoorthy *et al.*, Appl. Phys. Lett. **111**, 203502 (2017).
[7]A.-C. Liu, C.-H. Hsieh, C. Langpoklakpam, K. J. Singh, W.-C. Lee, Y.-K. Hsiao, R.-H. Horng, H.-C. Kuo, and C.-C. Tu, ACS omega **7**, 36070 (2022).
[8]T. Oshima, Y. Kato, N. Kawano, A. Kuramata, S. Yamakoshi, S. Fujita, T. Oishi, and M. Kasu, Appl. Phys. Express **10**, 035701 (2017).
[9]S. Pearton, F. Ren, M. Tadjer, and J. Kim, J. Appl. Phys. **124**, 220901 (2018).
[10]P. Ranga, A. Bhattacharyya, A. Chmielewski, S. Roy, R. Sun, M. A. Scarpulla, N. Alem, and S. Krishnamoorthy, Appl. Phys. Express **14**, 025501 (2021).
[11]J. Yang, S. Ahn, F. Ren, R. Khanna, K. Bevlin, D. Geerpuram, S. Pearton, and A. Kuramata, Appl. Phys. Lett. **110**, 142101 (2017).
[12]Y. Zhang *et al.*, Appl. Phys. Lett. **112**, 173502 (2018).
[13]B. Alhalaili, R. Vidu, H. Mao, O. Kamoun, and M. S. Islam, Ceram. Int. **47**, 479 (2021).
[14]S.-L. Ou, D.-S. Wuu, Y.-C. Fu, S.-P. Liu, R.-H. Horng, L. Liu, and Z.-C. Feng, Mater. Chem.Phys. **133**, 700 (2012).
[15]Y. H. Choi, K. H. Baik, S. Kim, and J. Kim, Appl. Surf. Sci. **539**, 148130 (2021).
[16]J. E. Hogan, S. W. Kaun, E. Ahmadi, Y. Oshima, and J. S. Speck, Semicond. Sci. Tech. **31**, 065006 (2016).
[17]H.-C. Huang, Z. Ren, C. Chan, and X. Li, J. Mater. Res. **36**, 4756 (2021).
[18]S. Jang, S. Jung, K. Beers, J. Yang, F. Ren, A. Kuramata, S. Pearton, and K. H. Baik, J. Alloys Compd. **731**, 118 (2018).
[19]Y. Kwon, G. Lee, S. Oh, J. Kim, S. J. Pearton, and F. Ren, Appl. Phys. Lett. **110**, 131901 (2017).
[20]H. Okumura and T. Tanaka, Jpn. J. Appl. Phys. **58**, 120902 (2019).
[21]A. P. Shah and A. Bhattacharya, J. Vac. Sci. Technol. A **35**, 041301 (2017).
[22]J. Yang, S. Ahn, F. Ren, S. Pearton, R. Khanna, K. Bevlin, D. Geerpuram, and A. Kuramata, J. Vac. Sci. Technol. B **35**, 051201 (2017).
[23]L. Zhang, A. Verma, H. G. Xing, and D. Jena, Jpn. J. Appl. Phys. **56**, 030304 (2017).
[24]Y. Zhang, A. Mauze, and J. S. Speck, Appl. Phys. Lett. **115**, 052102 (2019).
[25]C.-C. Chiang, X. Xia, J.-S. Li, F. Ren, and S. Pearton, Appl. Surf. Sci. **631**, 157489 (2023).
[26]S. J. Pearton, E. A. Douglas, R. J. Shul, and F. Ren, J. Vac. Sci. Technol. A **38**, 020802 (2020).
[27]X. Xia, N. S. Al-Mamun, D. Warywoba, F. Ren, A. Haque, and S. Pearton, J. Vac. Sci. Technol. A **40**, 053403 (2022).
[28]Y. K. Frodason, J. B. Varley, K. M. H. Johansen, L. Vines, and C. G. Van de Walle, Phys. Rev. B **107**, 024109 (2023).
[29]D. Hays, H. Cho, K. Jung, Y. Hahn, C. Abernathy, S. Pearton, F. Ren, and W. Hobson, Appl. Surf. Sci. **147**, 125 (1999).
[30]S. Salimian and C. Cooper III, J. Vac. Sci. Technol. B **6**, 1641 (1988).
[31]M. Beheshti and R. Westerman, AIP Adv. **11**, 025237 (2021).
[32]Y. Cai, G. Zhou, K. J. Chen, and K. M. Lau, IEEE Electr. Device L. **26**, 435 (2005).
[33]Y. Cai, Y. Zhou, K. M. Lau, and K. J. Chen, IEEE T. Electron Dev. **53**, 2207 (2006).
[34]T. Palacios, C. S. Suh, A. Chakraborty, S. Keller, S. P. DenBaars, and U. K. Mishra, IEEE Electr. Device L **27**, 428 (2006).
[35]J. C. Yang, C. Fares, F. Ren, R. Sharma, E. Patrick, M. E. Law, S. J. Pearton, and A. Kuramata, J. Appl. Phys. **123**, 165706 (2018).
[36]H. Mizuno, S. Kishimoto, K. Maezawa, and T. Mizutani, Phys. Status Solidi C **4**, 2732 (2007).
[37]P. P. Sundaram, F. Alema, A. Osinsky, and S. J. Koester, J. Vac. Sci. Technol. A **40**, 043211 (2022).
[38]D. B. Murin, I. A. Chesnokov, S. A. Pivovarenok, and A. M. Efremov, Russ. Microelectron. **52**, 1 (2023).